Strong Impact of Ionic Strength on the Kinetics of Fibrilar Aggregation of Bovine β-Lactoglobulin

Luben N. Arnaudov and Renko de Vries*

Laboratory of Physical Chemistry and Colloid Science, Wageningen University, Dreijenplein 6, 6700 EK Wageningen, The Netherlands and Food Physics Group, Wageningen University, Bomenweg 2, 6703 HD Wageningen, The Netherlands

Received June 19, 2006; Revised Manuscript Received September 20, 2006

We investigate the effect of ionic strength on the kinetics of heat-induced fibrilar aggregation of bovine β-lactoglobulin at pH 2.0. Using in situ light scattering we find an apparent critical protein concentration below which there is no significant fibril formation for all ionic strengths studied. This is an independent confirmation of our previous observation of an apparent critical concentration for 13 mM ionic strength by proton NMR spectroscopy. It is also the first report of such a critical concentration for the higher ionic strengths. The critical concentration decreases with increasing ionic strength. Below the critical concentration mainly "dead-end" species that cannot aggregate anymore are formed. We prove that for the lowest ionic strength this species consists of irreversibly denatured protein. Atomic force microscopy studies of the morphology of the fibrils formed at different ionic strengths show shorter and curvier fibrils at higher ionic strength. The fibril length distribution changes non-monotonically with increasing ionic strength. At all ionic strengths studied, the fibrils had similar thicknesses of about 3.5 nm and a periodic structure with a period of about 25 nm.

Introduction

The reversible formation of fibrils from globular proteins is a phenomenon occurring naturally, in vivo, for proteins such as actin and tubulin.[1] The irreversible formation of fibrils of various proteins is implicated in a number of debilitating diseases such as the Alzheimer's disease, Creutzfeldt−Jacob disease, systemic amyloidoses, and spongiform encephalopathies.[2] Almost all of the proteins that cause diseases by aggregation in vivo are found to also form fibrilar aggregates in vitro.[3] Moreover, many globular proteins not associated with diseases are also found to form fibrilar aggregates under specific conditions. For example, Gosal et al.[4] have recently shown that bovine β-lactoglobulin forms amyloid aggregates in solutions containing trifluoroethanol (TFE).

Another example of an irreversible fibril formation of globular proteins is provided by the fine-stranded heat-set gels formed by heating solutions of various globular food proteins such as ovalbumin,[5] bovine serum albumin,[6] and β-lactoglobulin.[7,8] The case of bovine β-lactoglobulin (β-lg) has been especially well studied. The bovine β-lg is of interest for the food industry because it is a major whey protein.[9] Also, because of its availability it is widely used for model protein studies. Equilibrium properties and heat-induced aggregation of β-lg have been extensively studied for a wide range of conditions (pH, ionic strength, and temperature).[10−19] Fine-stranded gels of β-lg are formed when heating at acidic pH.[7,8,20−23] Formation of β-lg fibrils at an acidic pH has been studied in considerable detail,[10−17] and yet, a detailed study of the effect of ionic strength on fibrilar aggregation of β-lg at pH 2.0 has not been performed.

Previously,[24] we studied the heat-induced fibril formation of β-lg at pH 2.0 and low ionic strength (13 mM) using light scattering (LS), proton nuclear magnetic resonance (NMR) spectroscopy, and atomic force microscopy (AFM). We found that fibril formation was a complex multistep process involving at least two routes—one leading to formation of long fibrils and a wastage reaction leading to a low molecular weight "dead-end" species that cannot aggregate anymore. Proton NMR indicates the presence of a critical aggregation concentration at about 2.5 wt %. It was argued that the critical concentration was a consequence of competition between fibril formation and the wastage reaction.

Despite previous studies, a number of unresolved issues remain: what is the nature of the "dead-end" species? And, given the known dependence of fibril formation on the pH and ionic strength, what is the role of the electrostatic interaction in the aggregation process? At least in part, elucidation of these issues is hampered by the lack of reliable kinetic data for the aggregation process. Modeling of such kinetic data could further contribute to a more detailed understanding of the aggregation process.

Previously, the kinetics of heat-induced aggregation of β-lg and the structure of the aggregates formed have been studied at pH 7.0[11,25−30] and 2.0.[10,24] The kinetics of fibril formation of β-lg at pH 2.0 has been studied by Aymard et al.[10] using static and dynamic light scattering as well as small angle neutron and X-ray scattering. Furthermore, using a precipitation technique they found that not all of the protein was converted to fibrils. Using a similar precipitation method, Veerman et al.[14] obtained similar results—only between 40% and 70% of the protein in the solution is converted into fibrils. This fraction was found to be independent of the ionic strength up to 0.08 M. In these studies, pH and temperature quenches are used to separate aggregates from monomers. We think that such an approach can lead to biased results—the studied system is taken too far from the state in which it has been during aggregation. Cooling of the solution and the pH quench inevitably change the physical state. Therefore, the results from the studies using that method do not reflect the real process even if we assume that what is

* To whom correspondence should be addressed. Phone: +31 (0)317-484561. Fax: +31 (0)317 483777. E-mail: Renko.deVries@wur.nl;

10.1021/bm060584i CCC: $33.50
Published on Web 11/09/2006

left in solution after the pH quench and precipitation of the aggregates is all the unreacted monomeric protein. Indeed, it is well known that denatured monomeric β-lg is precipitated by a pH quench.[31]

That is why the best approach to study the kinetics of protein aggregation is to use in situ experimental techniques as we do here. In the case of an in situ study the system is investigated during the process of aggregation *without introducing any change* in the conditions at which the aggregation occurs. Light scattering, small-angle X-ray, and neutron scattering as well as proton NMR spectroscopy are obvious candidates. We have used NMR and small angle neutron scattering previously in our investigations.[24,32]

Further structural information that can lead to a better mechanistic understanding of the formation of fibrils from a protein can be obtained by studying the morphology of the formed aggregates. The morphology of the aggregates formed by heating β-lg at acidic pH was studied by Kavanagh et al.[8] and Hamada and Dobson[15] by transmission electron microscopy. Atomic force microscopy (AFM) was used by Ikeda and Morris[16] to visualize fine-stranded (at pH 2.0) and particulate (at pH 7.0) β-lg and whey protein isolate (WPI) aggregates. AFM was also used in the study by Gosal et al.[4] to investigate fibrilar networks derived from β-lg in water or TFE−water solutions. A "beaded" appearance of the latter fibrils is observed. Aggregates formed by β-lg and whey protein isolates (WPI) at pH 2.0 were studied by Ikeda[17] using AFM and Raman scattering spectroscopy. The fine-stranded aggregates of β-lg appeared to be strings of monomers, whereas WPI aggregates were found to consist of granular aggregates.

With the aim of elucidating the role of the electrostatic interaction in the aggregation process and in order to obtain reliable kinetic data that may allow for kinetic modeling, we report here on a detailed in situ light scattering study of the aggregation process for various ionic strengths. There are quite a few complications in using light scattering to study the aggregation process: the fibrils that result from aggregation can be very long and start overlapping and interacting soon after the start of the reaction. This greatly complicates a quantitative interpretation of the light scattering data. Yet, there is always a time interval close to the start of the process during which the number and size of the aggregates is small enough such that one may assume that they are noninteracting. In this time window the scattering intensity may be expected to be proportional to the amount of aggregates. Therefore, we use here in situ light scattering to quantify the initial stage of the aggregation process.

We address the question of the nature of the "dead-end" species raised in our previous study.[24] We study in detail by AFM how the ionic strength influences the morphology of the fibrilar aggregates formed from β-lg water solutions at pH 2.0 upon heating at 80 °C and find that the length of the fibrils formed at different ionic strength shows a non-monotonic behavior. We also find that at low ionic strength the β-lg fibrils are long and straight, whereas at high ionic strength they are short and curvy.

Materials and Methods

Materials. Bovine β-lactoglobulin (β-lg) was obtained from Sigma (ref L0130, Lot 21K7079). It is a mixture of genetic variants A and B and used throughout all experiments. All solutions were prepared with deionized water (Barnstead) and contained 200 ppm NaN_3 to prevent bacterial growth. The pH was adjusted by addition of small amounts of 1 M HCl (Merck, Darmstadt, Germany). The ionic strength of the solutions was adjusted by addition of NaCl (Merck). Batch solutions were prepared from concentrated solutions of β-lg at pH 2.0 that were extensively dialyzed against 10 mM HCl solution. After dialysis the β-lg solutions were centrifuged for 3 h at 45 000*g* using a Beckman Avanti J-25I high-performance centrifuge and subsequently filtered through 0.45 μm low-protein adsorbing syringe filters (Sterile Acrodisk, Gelman Sciences) into the glass tubes in which the experiments were subsequently carried out. The solutions used in all experiments were prepared by dilution from the dialyzed ones. Care was taken to minimize dust. Glassware was cleaned with chromic acid, rinsed repeatedly with deionized water, and dried in a clean environment. The solutions for the light scattering experiments were filtered through 0.1 μm syringe filters (Sterile Acrodisk, Gelman Sciences) directly into the clean glass tubes prior to the experiments. The protein concentrations were determined by spectrophotometry at $\lambda = 278$ nm using an extinction coefficient of 0.83 $L \cdot g^{-1} \cdot cm^{-1}$.

Methods. *Light Scattering.* Static and dynamic light scattering data were obtained at a scattering angle of 90° using an ALV/SLS/DLS-5000 light scattering apparatus (Langen, Germany) equipped with an argon-ion laser (LEXEL, Palo Alto, CA) emitting vertically polarized light at a wavelength of 514.5 nm. The intensity of the scattered light was calibrated against the scattered light from pure toluene measured before each series of experiments at 25 °C. The scattering from the solvent was accounted for by subtracting the corresponding intensity from that of the protein sample. The absence of other than monomeric protein in the freshly prepared sample tubes was checked by dynamic light scattering at 25 °C for each sample. The aggregation process was then followed in situ by directly inserting the sample in the preheated sample holder of the LS setup which was at 80 °C, keeping it there for a period of time ranging from 1 to 24 h, while collecting scattering data, and subsequently quenching the sample in ice-cold water.

Because we are interested in the dependence of the amount of aggregated protein on the heating time especially for the early stages of the aggregation process, precise determination of the moment at which the heating commences is important. From previous studies[24] we know that aggregation begins when the heating temperature increases above 60 °C. To find the time dependence of the temperature in the sample cell we put a precise temperature sensor in a standard light scattering cell filled with 2 mL of water (the standard amount of solution we use in our experiments). Then we waited until the temperature was equilibrated to ambient temperature (~22 °C) and put the cell into the preheated to 80 °C light scattering apparatus while recording the temperature inside the cell with time. In about 100 s the temperature reached 70 °C, and we, therefore, chose that time as the time at which aggregation commences. This time coincides closely with the time at which the intensity of scattered light from β-lg solutions starts to increase.

(a) Background on Dynamic Light Scattering. DLS is a method that can be used to measure the mean size of scattering species in solution. In DLS one measures the intensity autocorrelation function

$$g_2(\tau,q) = \frac{\langle I(0,q)I(\tau,q)\rangle}{\langle I(0,q)\rangle^2} \tag{1}$$

where I is the scattered intensity, τ is the delay time, $q = (4\pi n/\lambda)\sin(\theta/2)$ is the wave vector, θ is the scattering angle, n is the refractive index of the solvent, and λ is the wavelength of the incident beam. The intensity autocorrelation function, g_2, is related to the field autocorrelation function g_1 by the Siegert relation

$$g_2(\tau,q) = 1 + \gamma|g_1(\tau,q)|^2 \tag{2}$$

In the latter equation γ is a positive proportionality constant smaller than or equal to unity, called a coherence factor.

For scattering from spherical monodisperse particles with radii R such that $qR \ll 1$, $g_1 \propto e^{-Dq^2t}$, where D is the diffusion coefficient of

the particles. In our case we start from a monomeric protein solution, which can be considered as a solution of fairly monodisperse spheres with a radius of about 2 nm. Once aggregation starts, larger particles are formed from the monomeric protein. In a rough approximation we can consider that we have some population of aggregates with some mean aggregation number coexisting with the rest of the protein monomers. For a scattering system containing two populations of monodisperse particles the simplest approach is to assume that g_1 has a biexponential decay[33]

$$g_1(t) = a_1 e^{-D_1 q^2 t} + (1 - a_1) e^{-D_2 q^2 t} \quad (3)$$

where D_1 and D_2 are diffusion coefficients of the relative species and a_1 and $1 - a_1$ are amplitudes that are proportional to the relative amount of scattering by particles of types 1 and 2. Effective hydrodynamic radii are calculated from the diffusion coefficients using the Stokes−Einstein relation

$$R_h = \frac{kT}{6\pi\eta D} \quad (4)$$

where k is the Boltzmann constant, T is the absolute temperature, and η is the viscosity of the solvent. Though we cannot directly use DLS to quantify the process of aggregation, we can have some indication whether in our aggregation process we reach some fixed aggregate size and the aggregates just grow in concentration or the aggregates grow in size and concentration with time.

Tapping Mode Atomic Force Microscopy. Tapping mode AFM was carried out by Nanoscope III, Multimode Scanning Force Microscope, Digital Instruments. For all experiments silicon tips for tapping mode in soft tapping conditions were used (Nanosensors, type NCH-W). To prepare samples for observation, protein solutions of different concentrations were put into tightly closed glass tubes and introduced in a water bath preheated at 80 ± 0.1 °C. At certain time intervals ranging from 1 to 48 h the tubes were taken out of the bath, aliquots were taken, and the tubes were returned into the bath. The aliquots were quenched in ice-cold water and diluted from the initial β-lg monomer concentration to a final protein concentration of 0.1 wt %. Protein dilution was done to facilitate quantitative comparison of the results obtained from the experiments performed at different initial protein concentrations. Protein monomers and/or protein aggregates were adsorbed on clean silicon substrates. The observations were performed on dry samples in air prepared as follows. The plates were cleaned first in pure ethanol by ultrasound and then rinsed with pure ethanol and dried with pure and dry nitrogen. The dry silicon plates were subsequently subjected to plasma cleaning. After the plasma cleaning the silicon plates were dipped into the test protein solutions for 1 h and then taken out, rinsed with a solvent at pH 2.0 containing no NaCl, and dried immediately by pure and dry nitrogen.

Results and Discussion

Dynamic Light Scattering. Figure 1 shows several autocorrelation functions corresponding to different heating times of a β-lg solution with a concentration of 4.73 wt % at pH 2.0 and 13 mM ionic strength. One can clearly see the time evolution of the curves due to the heat-induced protein aggregation. The lines through the experimental data are drawn by a least-squares fitting with a biexponential function (eq 3). Clearly, this simple approach describes well the experimental data for the initial stage of the aggregation. In Figure 2 the effective hydrodynamic radii corresponding to the two sets of relaxation times obtained from the fits illustrated in Figure 1 are shown. One can see that one of the radii stays virtually constant and equal to the hydrodynamic radius of the protein monomers, whereas the other, corresponding to the size of the formed aggregates, increases with heating time. It is worth noting that the intensity of the scattered light closely follows the form of the time dependence of the size of the aggregates. Figure 3 shows the amplitudes of the two exponents in eq 3 from the fits plotted in Figure 1. From the amplitude due to the aggregates it can be seen that the aggregates quickly dominate the scattering from the solution. Using the results from DLS

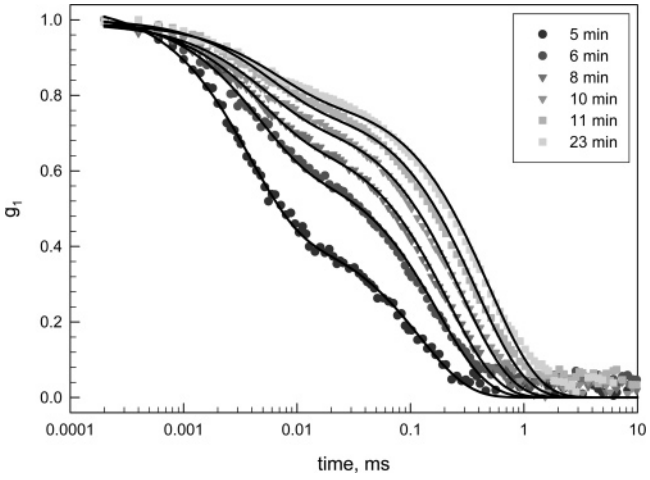

Figure 1. Field autocorrelation function for 4.73 wt % β-lg at pH 2.0 and 0.013 M ionic strength, heated at 80 °C for different heating times, indicated in the legend. The lines through the experimental points represent a biexponential best fit to the data.

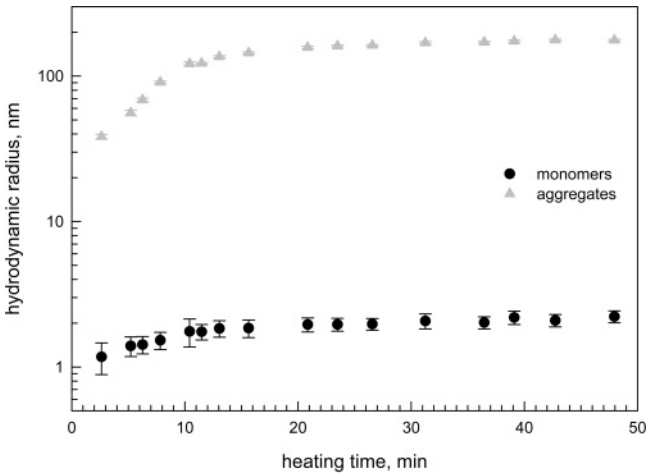

Figure 2. Hydrodynamic radii obtained from the biexponential fit to the data presented in Figure 1.

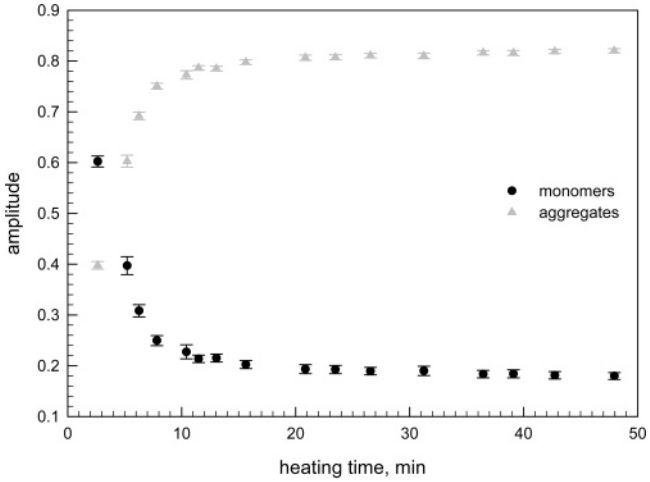

Figure 3. Dependence of the amplitudes from the biexponential fit shown in Figure 1 on the heating time.

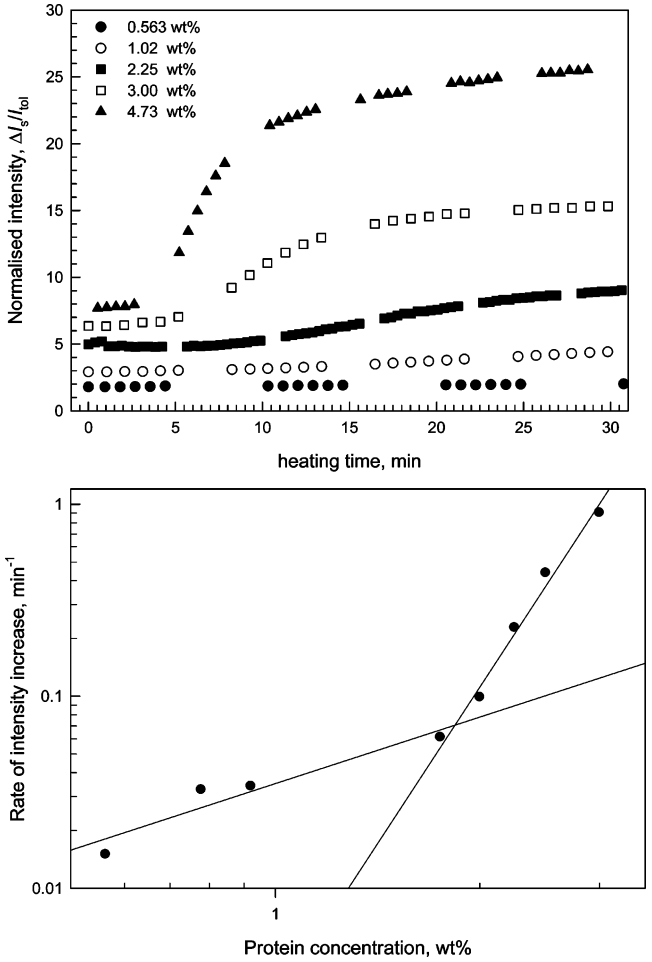

Figure 4. (a) Normalized scattered intensity of β-lg solutions at different concentrations at pH 2.0 and ionic strength $I = 0.013$ M as a function of heating time at 80 °C, as determined by LS. (b) Initial rate of increase of scattered intensity versus protein concentration for β-lg solutions at different concentrations at pH 2.0 and ionic strength $I = 0.013$ M, heated at 80 °C, as determined by LS.

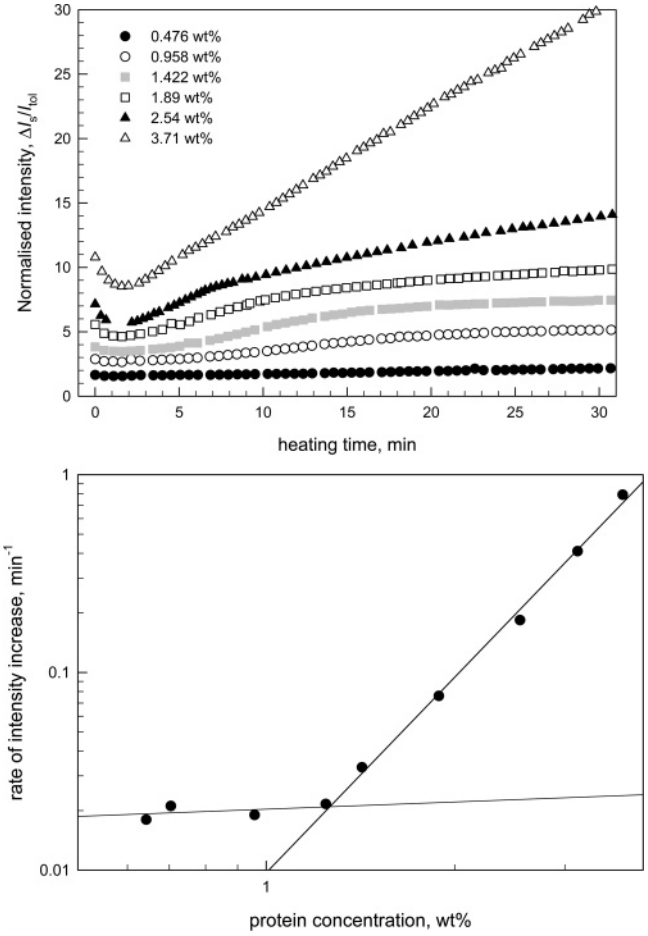

Figure 5. (a) Normalized scattered intensity of β-lg solutions at different concentrations, indicated in the legend, at pH 2.0 and ionic strength $I = 0.050$ M as a function of heating time at 80 °C, as determined by LS. (b) Initial rate of increase of scattered intensity versus protein concentration for β-lg solutions at different concentrations at pH 2.0 and ionic strength $I = 0.050$ M, heated at 80 °C, as determined by LS.

such as those plotted in Figure 2 we can estimate until what time we have a Rayleigh scattering regime. It appears that for our systems aggregate sizes are such that $qR < 1$ for the first 10−20 min of the aggregation process depending on the ionic strength and the initial protein concentration.

Further, we wanted to establish the nature of the β-lg which was not incorporated into fibrils after a prolonged heating. For that purpose we carried out the following set of experiments. First, we heated 1.5 mL of β-lg solution at pH 2.0 and a relatively high concentration (from 3.0 to 5.14 wt %) for 24 h at 80 °C. Second, we quenched the aggregation by inserting the test tube in ice-cold water. Because the sample had gelled, we subsequently diluted it to 3.5 mL with a solvent at pH 2.0 and left it to stay overnight at 4 °C. On the next day we took an aliquot for AFM and filtered the solution through a 0.1 μm filter directly into a clean light scattering cell. DLS from the resulting solution at ambient temperature showed the presence of only monomeric protein. For the case of 5.14 wt % β-lg solution the concentration of the filtered solution determined by spectrophotometry was 1.6 wt % due to both conversion of a part of the monomeric β-lg to fibrils and dilution. A subsequent heating of the filtered samples at 80 °C did not lead to any observable change in the mean hydrodynamic radius or the scattered intensity for as long as 5 h. An AFM image from the aliquots taken prior to the filtration showed the presence of fibrils in the heated solutions. All this, together with the NMR data from our previous study,[24] shows that the β-lg that is not taken up in the fibrils after prolonged heating is irreversibly denatured monomeric protein.

Static Light Scattering. The intensity of the scattered light from different β-lg samples at pH 2.0 and ionic strength of 13 mM inserted into a preheated at 80 °C LS apparatus is plotted in Figure 4a. The initial part of the curves in which the intensity is almost constant is due to a combination of effects involving mostly the process of temperature equilibration in the sample and, possibly, the initiation of the process of aggregation. After the initial temperature equilibration there is a region of a steep increase in the scattered intensity due to the aggregation process (see, e.g., the curve for 4.73 wt %). This region is best seen for concentrations higher than 2 wt %. Some time after the apparently linear region there is a crossover in the rate of increase of the scattered intensity and it becomes smaller. This crossover is possibly due to the fact that the dominating aggregate size becomes larger than q^{-1} and the scattering intensity becomes proportional to the number of large aggregates and not to their size. It is worth mentioning that the scattering intensity after the crossover also has an extended region which increases virtually linearly with heating time (see also the following data for other ionic strengths). The slope of the apparently linear region of the (normalized) intensity versus the heating time data can be used to extract more information about

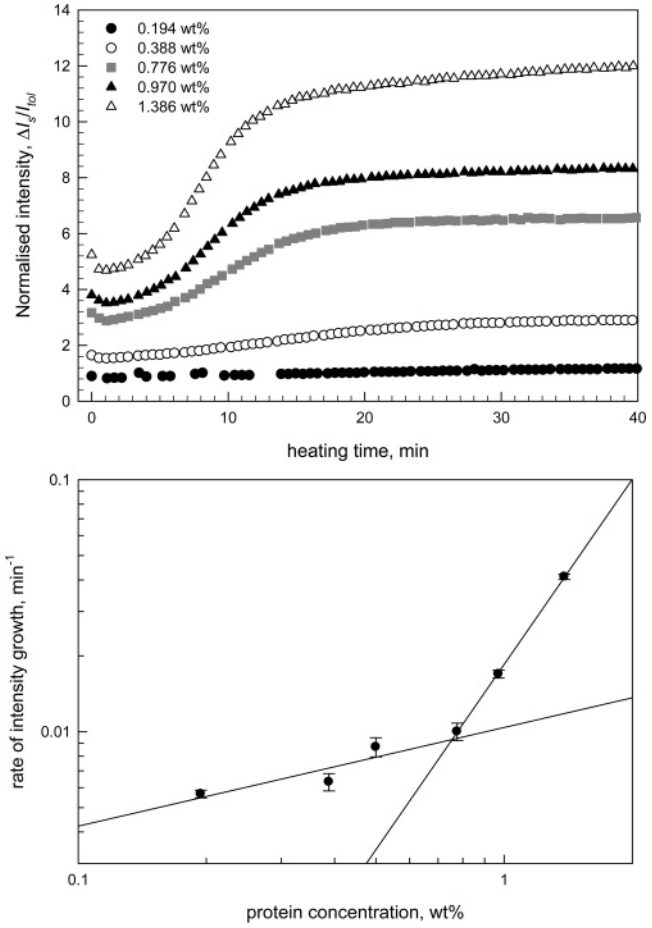

Figure 6. (a) Normalized scattered intensity of β-lg solutions at different concentrations, indicated in the legend, at pH 2.0 and ionic strength $I = 0.070$ M as a function of heating time at 80 °C, as determined by LS. (b) Initial rate of increase of scattered intensity versus protein concentration for β-lg solutions at different concentrations at pH 2.0 and ionic strength $I = 0.070$ M, heated at 80 °C, as determined by LS.

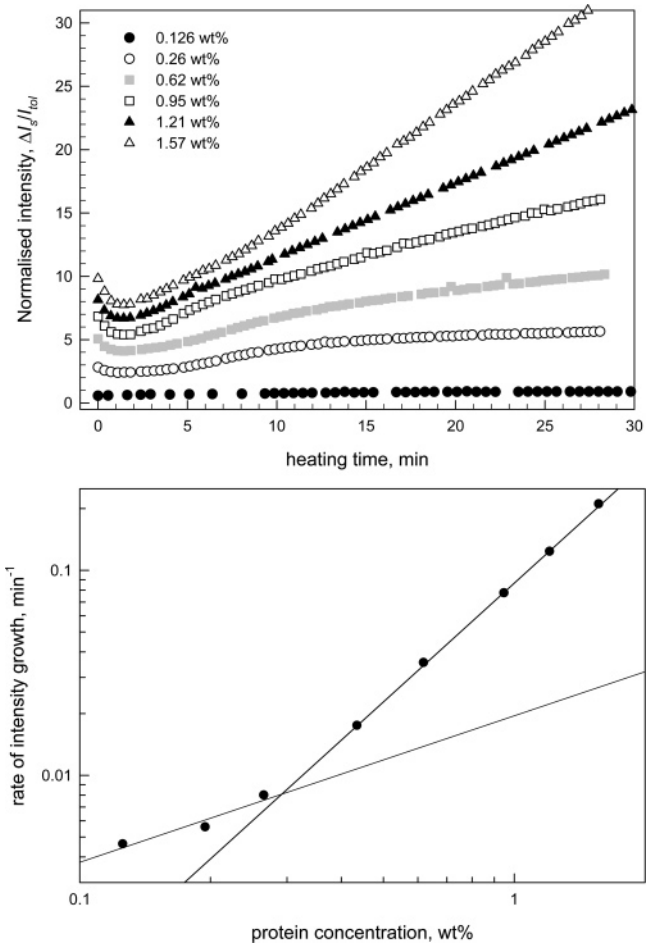

Figure 7. (a) Normalized scattered intensity of β-lg solutions at different concentrations, indicated in the legend, at pH 2.0 and ionic strength $I = 0.10$ M as a function of heating time at 80 °C, as determined by LS. (b) Initial rate of increase of scattered intensity versus protein concentration for β-lg solutions at different concentrations at pH 2.0 and ionic strength $I = 0.10$ M, heated at 80 °C, as determined by LS.

the kinetics of fibrilar aggregation of β-lg at pH 2.0: this quantity is proportional to the initial aggregation rate.

Figure 4b shows a plot of the initial rate of increase of the scattered intensity versus the protein concentration. The relative reproducibility of the rate determination for a fixed protein concentration is typically between 2% and 4%. In Figure 4b a relative error of 4% is smaller than the size of the symbols in the plot. For β-lg at pH 2.0 and ionic strength of 13 mM upon heating at 80 °C the change in the slope of the data plotted in Figure 4b indicates the presence of a critical aggregation concentration for fibril formation.

The value of the critical concentration for this case, obtained as the point of intersection between the linear regressions for the two distinct regions of the data, is 1.8 ± 0.5 wt %. The error in the critical concentration is estimated using an error propagation analysis based on the errors of the parameters obtained from the linear regressions. Interestingly enough, if we plot the rate of increase of the scattered intensity versus protein concentration for the linear region after the crossover we get a plot similar to the one shown in Figure 4b with a critical concentration of 2.1 ± 0.2 wt %, which is in good agreement with the result from the plot in Figure 4b. This result is in disagreement with the data of other researchers who either gave a lower critical value, 0.5 wt %,[10] or reported a final conversion (after 10 h of heating) depending on the initial protein concentration.[14] However, the value obtained by us is a result

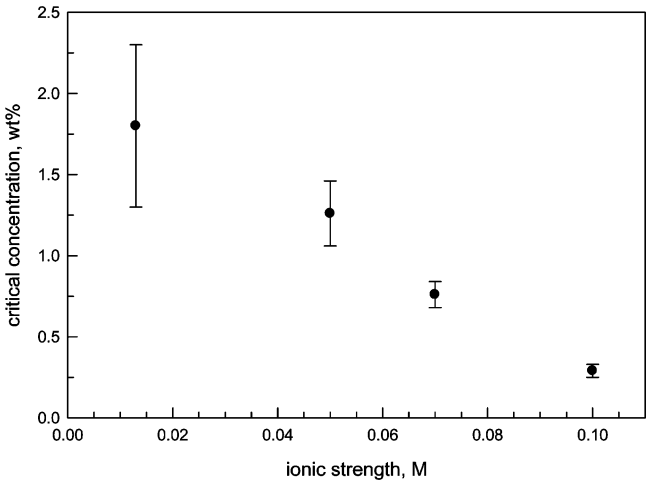

Figure 8. Critical aggregation concentration of β-lg as a function of the ionic strength.

of a very sensitive in situ experiment, whereas the data of the other authors result from a complicated procedure involving a pH quench with a subsequent precipitation, centrifugation, and spectrophotometric determination of the monomer concentration in the supernatant. In our opinion, the pH quench can lead to precipitation of not only the fibrils formed but also the denatured

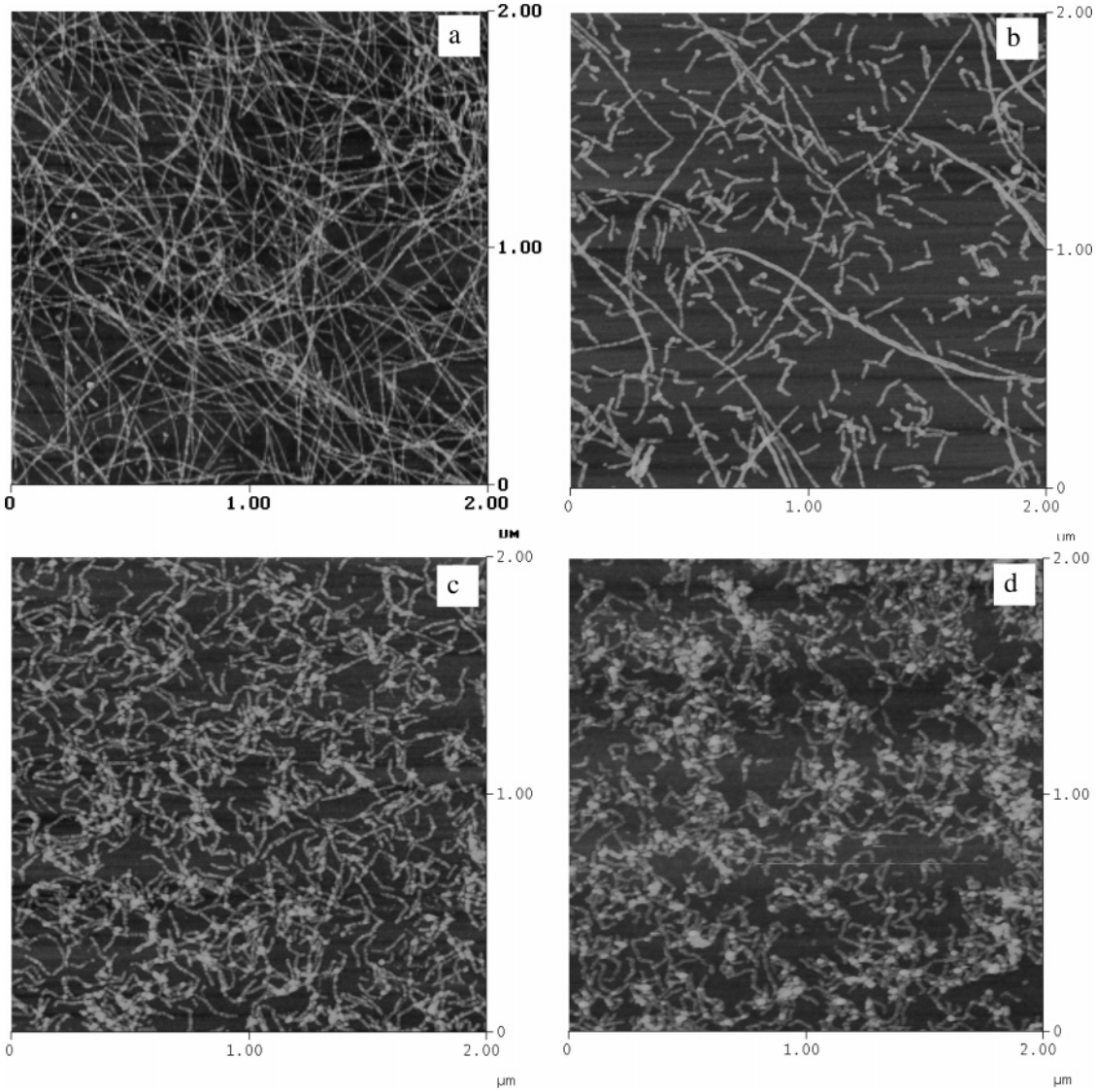

Figure 9. Tapping mode AFM height images of β-lg fibrils obtained after heating of β-lg solutions at pH 2.0 for 24 h at 80 °C at the following conditions: (a) 1.0 wt %, $I = 13$ mM; (b) 2.0 wt %, $I = 50$ mM; (c) 1.43 wt %, $I = 70$ mM; (d) 0.62 wt %, $I = 100$ mM.

single protein molecules, as previously reported by Harwalkar and Kalab.[31]

The results from the light scattering actually confirm a result from our previous work[24] where we have shown, using in situ proton NMR spectroscopy, that even after very long heating at pH 2.0 and 13 mM ionic strength a considerable amount of β-lg monomers is not incorporated into fibrils but left as monomers in solution. From the NMR data we estimated a critical concentration of about 2.5 wt %, in agreement with the LS data.

Next, we consider the changes in the aggregation process at higher ionic strengths. Figure 5a shows the intensity of the scattered light from different β-lg samples at pH 2.0 and ionic strength of 50 mM inserted into a preheated at 80 °C LS apparatus. The initial part of the curves first shows a decrease in the scattered intensity, which is most probably due to dissociation of the β-lg dimers present in the solution at that ionic strength. Indeed, if we plot the quantity Kc/R_θ at 25 °C, at a fixed scattering angle of 90°, as a function of the protein concentration, c, for different ionic strengths, we obtain straight lines that we can use to determine the molar mass of the scattering particles (data not shown). In Kc/R_θ K is an optical constant and R_θ is the Rayleigh ratio that is proportional to the scattered intensity. For 13 mM ionic strength the molar mass of the scattering particles obtained from the intercept of the plot is 17.5 ± 0.5 kDa, which is in good agreement with the molar mass of monomeric β-lg − 18.4 kDa. For 100 mM ionic strength the molar mass of the scattering particles obtained from the intercept of the plot is 40.0 ± 3 kDa, which is in good agreement with the molar mass of a β-lg dimer. It is also shown in the work of Aymard et al.[19] that the amount of β-lg dimers at pH 2.0 increases with increasing ionic strength and protein concentration and decreases with increasing temperature. The moment at which the intensity starts to increase coincides with the previously determined moment at which the temperature in the sample cell is increased above 70 °C (see Methods section), i.e., this increase is due to protein aggregation. One can see that the rate of intensity increase for the lower protein concentrations resembles the dependence observed at 13 mM ionic strength. With increasing concentration, however, the time dependence of the scattered intensity deviates from the one observed for lower concentrations: for the highest concentration it is practically linear for the entire observation time domain. The latter behavior is probably due to a coincidence in the aggregate formation rate and elongation rate of the protein fibrils. Using again the procedure followed for the data at 13 mM ionic strength, we plot the initial rates of increase of the

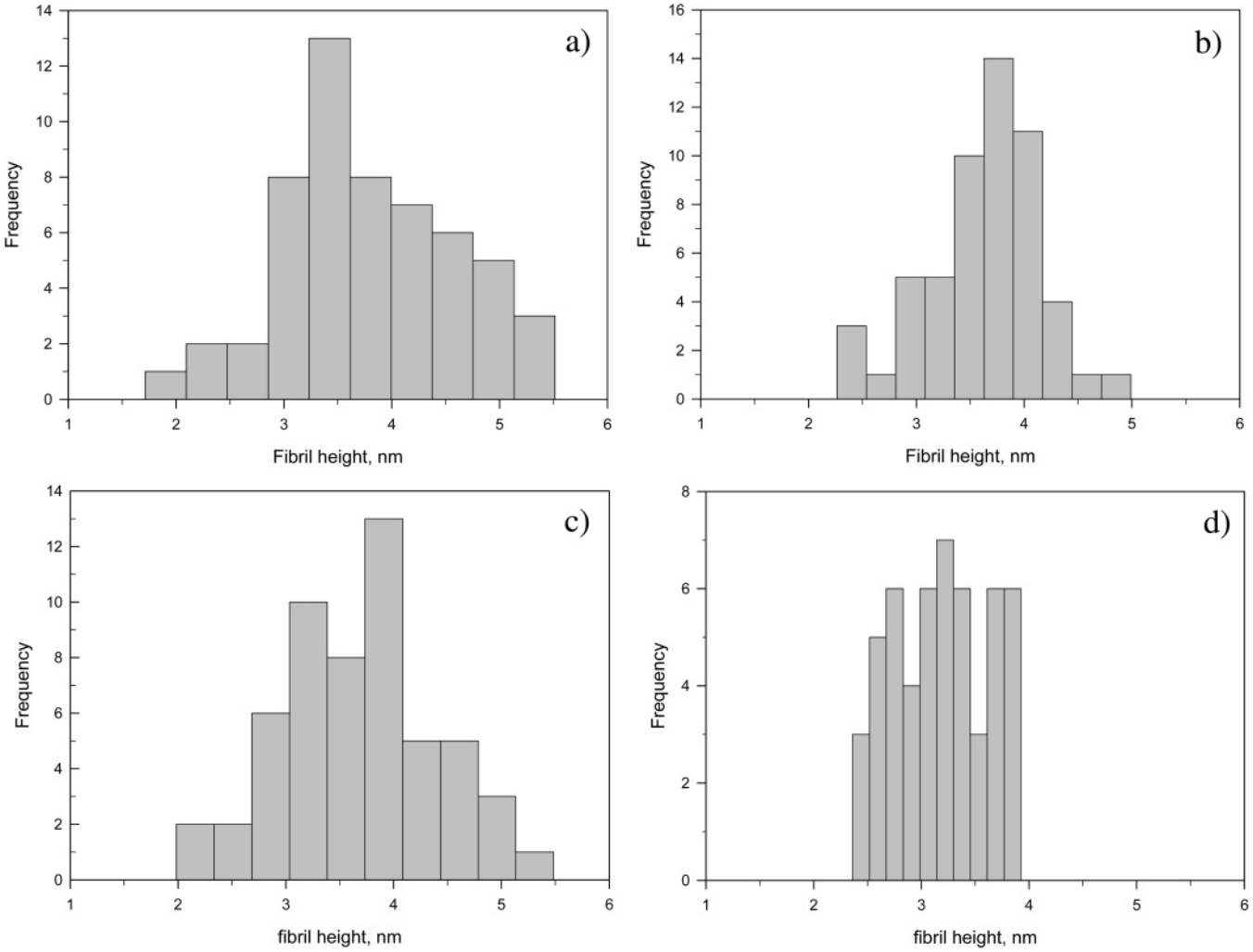

Figure 10. Height distribution of fibrils obtained by heating of β-lg solution at pH 2.0 at 80 °C and ionic strength of (a) 13, (b) 50, (c) 70, and (d) 100 mM.

scattered intensity as a function of protein concentration for experiments carried out at 50 mM ionic strength in Figure 5b.

The change in the slope of the data plotted in Figure 5b again indicates the presence of an apparent critical aggregation concentration for fibril formation for β-lg at pH 2.0 and ionic strength of 50 mM upon heating at 80 °C. The value of this critical concentration obtained by intersecting the linear regions of the data is 1.3 ± 0.2 wt %. The presence of a critical concentration and the similarity between the time dependence of the scattered intensity for experiments carried out at 13 and 50 mM ionic strength indicate that the generic kinetic scheme of fibril formation for this system is most probably one and the same for all ionic strengths; only the rate constants and, hence, the critical concentrations are ionic strength dependent.

Figures 6a and 7a show the scattered intensity of β-lg solutions at pH 2.0 and ionic strength of 70 and 100 mM, respectively. The dependence of the scattered intensity on the heating time is similar to the one at lower ionic strengths (see Figures 4a and 5a). The effect of monomer−dimer equilibrium is most pronounced at 100 mM ionic strength (see Figure 7a). The corresponding rates of the initial increase of the scattered intensity for 70 and 100 mM ionic strength are plotted in Figures 6b and 7b. The characteristic change of the slope due to the presence of a critical concentration is observed in both figures. The values of the critical concentrations, obtained in the same way as in Figures 4b and 5b, are 0.76 ± 0.08 wt % for 70 mM ionic strength and 0.29 ± 0.04 wt % for 100 mM ionic strength. The dependence of the critical concentrations on the ionic strength is plotted in Figure 8. The critical concentration depends strongly on the ionic strength: for an increase of the ionic strength with about an order of magnitude the critical concentration decreased by about an order of magnitude too.

Obviously, the key factor causing that behavior is the electrostatic interaction. At pH 2.0 every β-lg molecule has approximately 20 positive charges. At 13 mM ionic strength the electrostatic repulsion is not entirely screened (Debye length ≈ 3 nm > the radius of the protein molecule ≈ 2 nm) and the aggregation process is slow, which leads to a large amount of protein going into an inactive state via denaturation. The nucleation and elongation of fibrilar aggregates are processes involving two or more protein molecules and presumably more sensitive to ionic strength than protein denaturation, which is a monomolecular process. With increasing ionic strength the electrostatic repulsion is screened to a greater extent and the aggregation process (fibril nucleation and/or elongation) becomes faster, thus leading to a smaller amount of denatured monomeric protein and a lower critical concentration. A similar effect of the balance between nucleation and elongation rate is observed by Lomakin et al.[34] for the case of amyloid β-protein. Below some critical concentration only a small number of nuclei are formed, the elongation rate dominates, and very long fibrils are formed. Above the critical concentration the nucleation rate is comparable to the elongation rate and short fibrils are formed.

In our case, it could be expected that at a sufficiently high

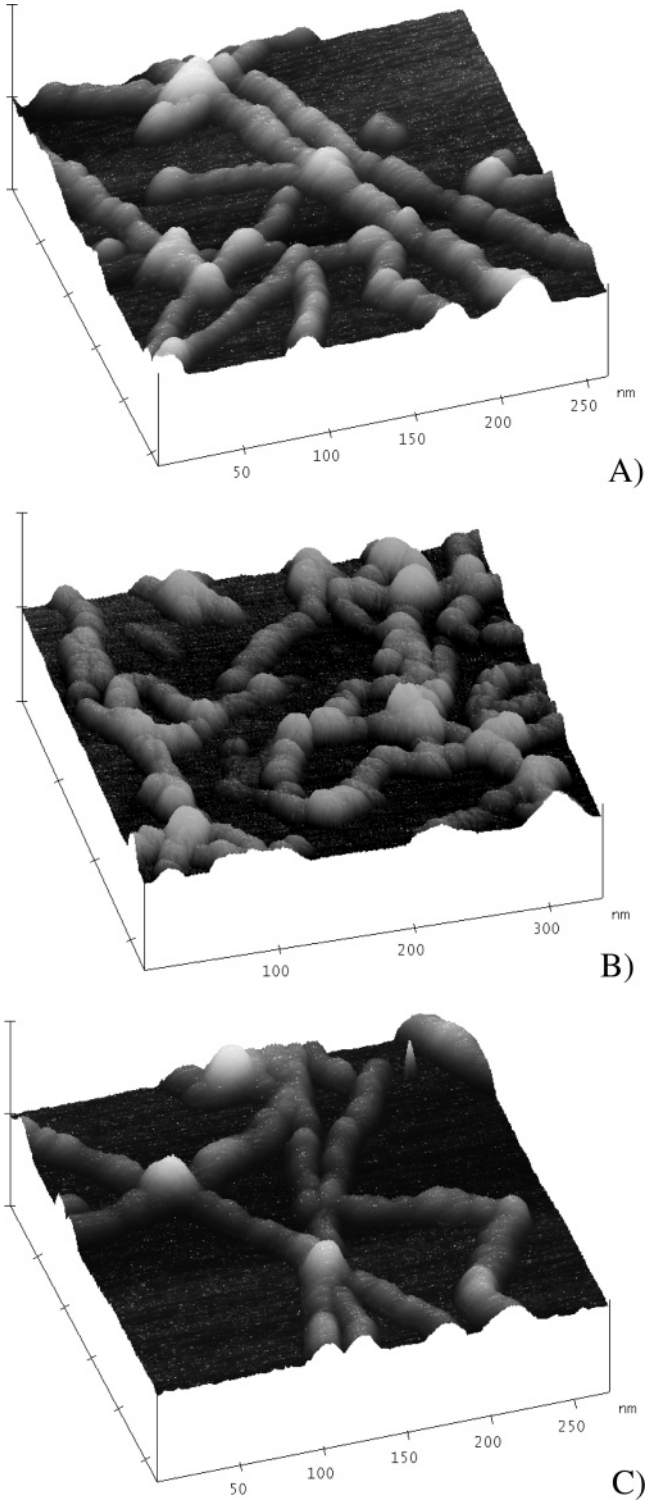

Figure 11. 3D projections of AFM tapping mode height images of fibrils obtained after heating of β-lg solutions at pH 2.0 and ionic strength of (A) 50, (B) 70, and (C) 100 mM. The height scale is 10 nm for all pictures.

ionic strength there would no longer be a critical concentration and all the protein would go into aggregates. Determination of such a limit using light scattering is impractical because it would require measurements at protein concentrations lower than 0.1 wt %.

If we combine the information obtained from the in situ light scattering experiments with the information obtained form our previous study,[24] the following simple reaction scheme emerges. Upon heating of a β-lg solution at pH 2.0 at 80 °C, the protein molecules partially unfold, which may be considered as an activation step. An unfolded molecule is either attached to another unfolded molecule or completely denatured. Obviously, denaturation must be a first-order reaction with a rate constant which may or may not depend on the ionic strength. Aggregation probably occurs through a nucleation and growth mechanism, but the size of the nucleus can only be determined by comparing with a kinetic model.[35]

Atomic Force Microscopy. Figure 9a, b, c, and d shows tapping mode AFM height images of β-lg fibrils obtained upon heating aqueous solutions at pH 2.0 at 80 °C and ionic strengths of 13, 50, 70, and 100 mM, respectively. As can be easily seen, the morphology of the fibrils formed is strongly affected by the ionic strength of the solutions. The fibrils obtained at 13 mM ionic strength are long and straight, whereas the fibrils obtained at 100 mM ionic strength are short and curly, in agreement with previous reports.[4,10,16] A similar dependence on the ionic strength has also been observed for ovalbumin by Cryo-TEM.[36] In our case, the effect of the ionic strength seems to be non-monotonic, since one can still observe long and straight fibrils at an ionic strength of 50 mM, whereas the fibrils obtained at 70 and 100 mM ionic strength are short and curved. The coexistence of short and long fibrils at 50 mM ionic strength (Figure 9b) further complicates the aggregation scenario. The possibility that at an intermediate ionic strength more steps exist in the aggregation kinetics of β-lg is an interesting task for a future investigation.

The ionic strength affects only the (average) length and shape of the fibrils but not their thickness (height). Figure 10a−d shows the size distribution of the thickness of fibrils obtained at different ionic strengths, measured from the height of the fibrils from the AFM images. The corresponding fibril thicknesses are 3.8 ± 0.7 nm for $I = 13$ mM, 3.6 ± 0.5 nm for $I = 50$ mM, 3.7 ± 0.7 nm for $I = 70$ mM, and 3.3 ± 0.3 nm for $I = 100$ mM. Clearly, the thicknesses of the fibrils obtained at different ionic strengths coincide within the experimental error.

At all ionic strengths studied the fibrils exhibit a periodic structure with a periodicity between 22 and 28 nm (see Figure 11). This periodicity varies between different fibrils within the same sample and is apparently independent of the ionic strength in the studied range. Irregular periodicity is reported also by Aymard et al.[10] and can be noticed in a number of AFM images of β-lg fibrils obtained by different authors at different conditions.[4,16,17] Most likely, the fibrils have a helical organization. Helicity is easily observed in AFM pictures of much thicker amyloid fibrils. Recently, using super sharp tips, we have also been able to show using AFM that thin, heat-induced lysozyme fibrils are helical.[37]

Conclusions

We studied the kinetics of heat-induced aggregation of β-lg at pH 2.0 and various ionic strengths by in situ light scattering and showed that there are apparent critical concentrations for fibril formation at all ionic strengths studied. The critical concentration decreases with increasing ionic strength. This shows that the electrostatic repulsion between the protein monomers is the key factor determining the rate of fibril formation. The nucleation and elongation of protein fibrils, being multimolecular reactions, depend more strongly on the ionic strength than denaturation, which is a monomolecular reaction. In other words, more screening of the electrostatic interaction results in faster aggregation. This is qualitatively consistent with the AFM studies on samples taken from β-lg solutions at pH

2.0 and different ionic strengths. Fibrils obtained at a higher ionic strength are shorter and more curved as opposed to the longer and straighter fibrils obtained at lower ionic strengths. It seems that at a higher ionic strength fibril nucleation is faster, more fibrils are formed, and as a result the mean length of the fibrils is shorter. At the same time, fibrils obtained at all ionic strengths in our study exhibit a similar type of periodic morphology, which suggests that the molecular mechanism of fibril formation is most likely independent of the ionic strength but specific for this protein. By combination of static and dynamic light scattering and filtration of the aggregated solution we have also shown that the "dead-end" species observed by us in a previous study[24] is irreversibly denatured β-lg monomer.

Acknowledgment. This work was supported by The Netherlands Research Council for Chemical Sciences (CW) with financial aid from The Netherlands Organization for Scientific Research (NWO) in the context of the SOFTLINK program "Theoretical Biophysics of Proteins in Complex Fluids".

References and Notes

(1) Oosawa, F.; Asakura, S. *Thermodynamics of Polymerization of Protein*; Academic Press: New York, 1975.
(2) Dobson, C. M. *Philos. Trans. R. Soc. Lond*on **2001**, *B 356*, 133.
(3) *(3) Chamberlain, A. K.; MacPhee, C. E.; Zurdo, J.; Morozova-Roche, L. A.; Hill, H. A. O.; Dobson, C. M.; Davis, J. J. Biophys. J.* **2000**, *79*, 3282.
(4) Gosal, W. S.; Clark, A. H.; Pudney, P. D. A.; Ross-Murphy, S. B. *Langmuir* **2002**, *18*, 7174.
(5) Koike, A.; Nemoto, N.; Doi, E. *Polymer* **1996**, *37*, 587.
(6) Lefebvre, J.; Renard, D.; Sanches-Gimeno, A. C. *Rheol. Acta* **1998**, *37*, 345.
(7) Langton, M.; Hermansson, A.-M. *Food Hydrocolloids* **1992**, *5*, 523.
(8) Kavanagh, G. M.; Clark, A. H.; Ross-Murphy, S. B. *Int. J. Biol. Macromol.* **2000**, *28*, 41.
(9) Wong, D. W. S.; Camirand, W. M.; Pavalath, A. E. *Crit. Rev. Food Sci. Nutr.* **1996**, *36*, 807.
(10) Aymard, P.; Nicolai, T.; Durand, D.; Clark, A. H. *Macromolecules* **1999**, *32*, 2542.
(11) Le Bon, Ch.; Nicolai, T.; Durand, D. *Macromolecules* **1999**, *32*, 6120.
(12) Lefevre, T.; Subirade, M. *Biopolymers* **2000**, *54*, 578.
(13) Schokker, E. P.; Singh, H.; Pinder, D. N.; Creamer, L. K. *Int. Dairy J.* **2000**, *10*, 233.
(14) Veerman, C.; Ruis, H.; Sagis, L. M. C.; van der Linden, E. *Biomacromolecules* **2002**, *3*, 869.
(15) Hamada, D.; Dobson, C. M. *Protein Sci.* **2002**, *11*, 2417.
(16) Ikeda, S.; Morris, V. J. *Biomacromolecules* **2002**, *3*, 382.
(17) Ikeda, S. *Spectrosc. Int. J.* **2003**, *17*, 195.
(18) Verheul, M.; Pedersen, J. S.; Roefs, S. P. F. M.; de Kruif, K. G. *Biopolymers* **1999**, *49*, 11.
(19) Aymard, P.; Durand, D.; Nicolai, T. *Int. J. Biol. Macromol.* **1996**, *19*, 213.
(20) Tobitani, A.; Ross-Murphy, S. B. *Macromolecules* **1997**, *30*, 4845.
(21) Tobitani, A.; Ross-Murphy, S. B. *Macromolecules* **1997**, *30*, 4855.
(22) Kavanagh, G. M.; Clark, A. H.; Ross-Murphy, S. B. *Langmuir* **2000**, *16*, 9584.
(23) Renard, D.; Lefebvre, J. *Int. J. Biol. Macromol.* **1992**, *14*, 287.
(24) Arnaudov, L. N.; de Vries, R.; Ippel, H.; van Mierlo, C. P. M. *Biomacromolecules* **2003**, *4*, 1614.
(25) Le Bon, C.; Nicolai, T.; Durand, D. *Int. J. Food Sci. Technol.* **1999**, *34*, 451.
(26) Gimel, J. C.; Durand, D.; Nicolai, T. *Macromolecules* **1994**, *27*, 583.
(27) Verheul, M.; Roefs, S. P. F. M.; de Kruif, K. G. *J. Agric. Food Chem.* **1998**, *46*, 896.
(28) Hoffmann, M. A. M.; Roefs, S. P. F. M.; Verheul, M.; van Mil, P. J. J. M.; de Kruif, K. G. *J. Dairy Res.* **1996**, *63*, 423.
(29) Hoffmann, M. A. M.; van Mil, P. J. J. M. *J. Agric. Food Chem.* **1997**, *45*, 2942.
(30) Hoffmann, M. A. M.; van Mil, P. J. J. M. *J. Agric. Food Chem.* **1999**, *47*, 1898.
(31) Harwalkar, V. R.; Kalab, M. *Milchwissenschaft* **1985**, *40*, 665.
(32) Arnaudov, L. N.; de Vries, R.; Cohen Stuart, M. A. *J. Chem. Phys.* **2006**, *124*, 084701.
(33) Berne, B. J.; Pecora, R. *Dynamic Light Scattering: With Applications to Chemistry, Biology, and Physics*; Dover Publications, Inc.: New York, 2000.
(34) Lomakin, A.; Chung, D. S.; Benedek, G. B.; Kirschner, D. A.; Teplow, D. B. *Proc. Natl. Acad. Sci. U.S.A.* **1996**, *93*, 1125.
(35) Ferrone, F. *Methods Enzymol.* **1999**, *309*, 256.
(36) Pouzot, M.; Nicolai, T.; Visschers, R. W.; Weijers, M. *Food Hydrocolloids* **2005**, *19*, 231.
(37) Arnaudov, L. N.; de Vries, R. *Biophys. J.* **2005**, *88*, 515.

BM060584I